19/04/2024 16:47

(Article begins on next page)

Author's Accepted Manuscript

Surface properties of new green building material after TiO$_2$-SiO$_2$ coatings deposition

Rosa Taurino, Luisa Barbieri, Federica Bondioli
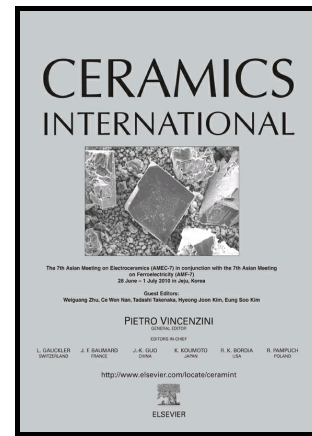
Cite this article as: Rosa Taurino, Luisa Barbieri and Federica Bondioli, Surface properties of new green building material after TiO$_2$-SiO$_2$ coatings deposition, *Ceramics International,* http://dx.doi.org/10.1016/j.ceramint.2015.12.002

Surface properties of new green building material after TiO_2-SiO_2 coatings deposition

Rosa Taurino[a*], Luisa Barbieri[b], Federica Bondioli[a,c]

[a]Dipartimento di Ingegneria Industriale, Università degli studi di Parma, Parco Area delle Scienze 181/A, 43124 Parma (I)

[b]Dipartimento di Ingegneria "Enzo Ferrari", Università degli studi di Modena e Reggio Emilia, Via Vivarelli 10, 41125 Modena (I)

[c]Consorzio Interuniversitario Nazionale per la Scienza e Tecnologia dei Materiali (INSTM), Via G. Giusti 9, 50121 Firenze (I)

Corresponding author:

*Rosa Taurino, Dipartimento di Ingegneria Industriale, Università degli studi di Parma, Parco Area delle Scienze 181/A, 43124 Parma (I), tel: + 39 0521 906355, fax: +39 0521 905705, email address: rosa.taurino@unipr.it

Abstract

The aim of this study was the surface functionalization of a new green ceramic material, obtained using packaging glass waste (PGW), to improve its cleanability. This objective was reached through the deposition by air-brushing of a nanostructured coating based on titania-silica sol-gel suspension. The coatings were deposited on both glazed and unglazed ceramic substrates and the thermal treatment conditions (temperature) were optimized. The obtained results suggest that the applied coatings are transparent and show a good scratch resistance and photocatalitic activity under the tested conditions. The photodegradation process and the mechanical properties are clearly affected by the thermal treatment and thus by the sample surface roughness. The best surface properties were obtained with a thermal treatment at temperature of 150°C. These coatings do not

1

exhibit either cracks from the substrate. All in all, the developed surface modified

ceramic material is attractive as potential sustainable building material.

Keywords: TiO$_2$; Sol-gel process; Functional application.

1. Introduction

In an environmental context, the construction industry has a major impact on

sustainable development. As known, the construction sector has major impacts on all

three pillars of sustainable development: environment, society, and economy [1, 2]. In

fact, it has some of the biggest direct effects on water, resources, land use, and

greenhouse gas emissions [2, 3], and some indirect effects on the environment affecting

transport and, as consequence, communities and public health [4, 5]. For such reasons,

the environmental issues in the construction industry are reduction of raw material

extraction and consumption, land-use change, including clearing of existing flora,

energy use and associated emissions of greenhouse gases, aesthetic degradation, water

use, waste water generation, etc [4].

In this context, the development of innovative materials based on huge amount of

alternative raw materials deriving from waste matter recovery and with self-cleaning

properties can be a significant step towards the reduction of the environmental impact of

this sector. One category of waste that can be considered as new raw material for

ceramic and building sector is the glass waste coming from packaging glass (PGW)

collected by urban separated collection. In fact, according to data reported by CoReVe,

the Italian Consortium for the collection, recycling and reuse of packaging glass waste,

approximately 2.186.300 tons of packaging glass were put on market in 2013, the 73%

of which was collected by separate collection. In other words, around 1.596.000 tons of

the packaging glass are recovered mainly in glassworks (99%) and 1% in alternative recovery (ceramic industry, building, other glass sectors) [6]. The potential use of this alternative raw material in the production of new ceramic materials has already been evaluated by Barbieri et al. [7, 8]. These studies showed the feasibility to use the glass waste (PGW) for the manufacture by lamination process of a new green material, having a composition quite different from the traditional ceramic tiles, building bricks and roof tiles. If several works studied the possibility to use the glass waste as new fluxing agent in replacement of traditional feldaspar [9, 10, 11], in these studies Barbieri et al. showed the possibility to obtain a new ceramic material where feldaspar and quartz sand are completely replaced. The new ceramic material, based on a huge amount of glass waste (80wt%) and 20wt% of refractory clay, sinter at low temperature (950°C) and can be used as wall and floor coverings [7, 8]. As a consequence, this new kind of ceramic tiles can save energy, due to the reduction of sintering temperatures, and raw materials, due to the very low amount of used clay. However, the high porosity and thus the high dirtiness represent significant drawbacks of this innovative material, making necessary a periodical surface cleaning process, that has as a result the altering of the surface aesthetic aspect, or a glazed coating. The protection of the ceramic material is therefore a serious challenge in building material. In order to improve surface cleanability properties of ceramic materials the photocatalycity of titanium dioxide (TiO_2) nanoparticles can be used [12]. TiO_2 is widely used in different materials and applications: exterior construction materials [13, 14], water [15] and air purification [16], self-cleaning and antibacterial cement mortar [17], tiles [18], glass [19], and, recently, cultural heritage[20]. In fact anatase titania polymorph is a photocatalyzer that, when exposed to radiation of adequate wavelength, is able to catalyze the mineralization

of polluting agents, either organic and inorganic, as well as to show superhydrophilicity and antibacterial properties [16, 18, 21].

Taking into account the idea of exploiting the transparency of coatings, in this work the authors evaluated the possibility to obtain a multifunctional surface for the new green ceramic material obtained using a high amount of packaging glass waste (PGW), using TiO_2-SiO_2 based sol-gel coatings. Infact, as showed by other research papers, [18, 20, 22], TiO_2-SiO_2 binary films, deposited by air-brushing on fired tiles, allowed to obtain higher adhesion and self-cleaning properties.

TiO_2-SiO_2 films were prepared depositing by air-brushing a colloidal solution of titania nanoparticles on the surface of the green material. The modification of the TiO_2-SiO_2 coatings with $AgNO_3$ was also investigated to assure the antibacterial activity of the coating in any illumination conditions [23]. In fact, silver is so far one of the best known antimicrobial/antifungal agent due to a strong cytotoxic effect not restricted by UV illumination toward a broad range of microorganisms and due to its remarkably low human toxicity compared with other heavy metal ions. The films, deposited on both glazed and unglazed ceramic substrates, were characterized to mainly evaluate the effect of the thermal treatments and $AgNO_3$ addition on photocatalycity and coating mechanical properties. In fact, another general purpose of this coating is to protect and then to enhance the appearance and durability of the substrate. Therefore, coating properties such as adhesion and scratch resistance are critical and have to be enhanced retaining at the same time the basic functions of the specific coating [24].

2. Material and methods

2.1 Coating preparation and deposition

The material selected for evaluating the efficiency of TiO_2-SiO_2 based coatings was an innovative ceramic material where feldaspar and quartz sand are completely replaced by

80 wt% of PGW and 20 wt% of kaolin ceramic grade, and manufactured by lamination process.

To prepare suitable prismatic specimens (5.0 x 5.0 x 1.0 cm^3), the raw materials were ground and sieved below 500 μm [7]. The milled powders were mixed with a water-soluble binding polymer (8 wt%), homogenized, and formed by lamination. The compacts were dried at 60°C and then fired in an electrical laboratory furnace (model AWF 13/12, Lenton, Hope Valley, U.K.), at a firing temperature of 950°C with 15 min of soaking time.

Total porosity (P_t) was evaluated by the difference between absolute density, ρ_{ab}, and apparent density, ρ_a, of ceramics (Eq. 1);

$$Pt(\%) = \frac{\rho_{ab} - \rho_a}{\rho_{ab}} \times 100 \qquad (1)$$

where ρ_a was estimated by a dry flow Pycnometer (Micromeritics GeoPyc 1360) using a bulk sample of 1 x 1 cm^2, while ρ_{ab} by a He displacement Pycnometer (Micromeritics ACCUPYC 1330), after crashing and milling the samples below 45 μm. The total porosity of the so obtained ceramic material was 27%.

In order to evaluate the effect of the TiO_2-SiO_2 functional coating also as protective layer, the coating was applied both on unglazed and glazed ceramic. The commercial transparent glaze was supplied by Colorobbia Spa and deposited on the green ceramic substrate before its sinterization. In particular the glaze, coded CLA3, was chosen for its coefficient of thermal expansion (5.9x10^{-6} C^{-1}) and for its firing temperature (930-970°C) in good dilatometric agreement with that of the substrate (7.5x10^{-6} C^{-1}). The glazed and unglazed samples were sintered in an electric laboratory furnace (Nambertherm) at 10°C/min heating rate and 1 h of soaking time at 950°C.

For glazed and unglazed samples the surface porosity (P_S) was estimated as reported in Eq.2 [25];

$$Ps(\%) = \frac{\rho_s - \rho_a}{\rho_{ab}} \times 100 \qquad (2)$$

where skeleton density, ρ_s, was measured by a He displacement Pycnometer (Micromeritics ACCUPYC 1330), on the obtained samples, while ρ_{ab} and ρ_a were measured as already reported. The surface porosity of unglazed and glazed samples was about 22% and 0.5% respectively.

On the obtained specimens, the titania-silica sol (titania content 2wt%) was deposited by spray coating at room temperature, using an air brush at a pressure of 6-8 bar, at a distance of about 14 cm from the substrate. Each sample was coated with a unique spray cycle with 0.24 ml/cm^2 of solution with an average TiO_2 content of about 48 g/m^2. For every single spray were used about 6 ml of sol. Table 1 reports the chemical composition of the used titania-silica sol. Finally, the effect of $AgNO_3$ addition (0.25 g for each liter of titania sol) on the TiO_2-SiO_2 based coatings was also investigated. After the deposition, the samples were dried at 30°C overnight and treated at different temperature (25, 150 and 300°C) and treatment time to evaluate the effect on the mechanical properties and on the photocatalytic efficiency of the sol-gel coatings. Table 2 reports the sample codes and the experimental conditions evaluated.

2.2 Sample characterization

The effect of the coating on the material color was determined by performing color measurements on both uncoated and coated tiles by the CIELAB method to get L*, a*, and b* values.

According to UNI EN 15801 [26] color change, ΔE*, between two different surfaces is defined as:

$$\Delta E^* = \sqrt{(\Delta L^*)^2 + (\Delta a^*)^2 + (\Delta b^*)^2} \qquad (3)$$

where in the CIELAB notation ΔL* is the change in lightness, Δa* and Δb* the change in hue (a* is the red (>0) green (<0) coordinate and b* the yellow (>0) blue (<0) coordinate). The result was the mean of 3 measurements on 6 different specimens for each different typology of substrate.

The photocatalytic activity of the coatings was evaluated by colorimetric analysis using the standard rhodamine B (RhB) photo-degradation test. The dye (water solution containing 0.05 ± 0.005 g/l of rhodamine B) was applied on both treated and untreated samples using a syringe (0.5 ml deposited in a 22 ± 2 cm^2 area for each specimen). After 24 h long drying phase in the dark at room temperature, colorimetric measurements were carried out to establish color changes due to the dye on stained part of the sample. Afterwards the samples were exposed to UVA light (irradiance value on tile surfaces: 3.75 ± 0.25 W/m^2) as reported by UNI 11259 [27]. The photoinduced decomposition of rhodamine B during time was monitored by a portable colorimeter (Konica Minolta CM 2600 D) after 4 and 26 h of UV light exposure. Only chromatic coordinate a* of CIELAB color space was used to determine the photocatalytic discoloration of stain after 4 and 26 hours of UV irradiation as:

$$R(t) = \frac{a^*(0) - a^*(t)}{a^*(0)} \times 100 \qquad (4)$$

where a*(0) and a*(t) are the measured values of a* before and after t hours of UV irradiation exposure, respectively. The photocatalytic discoloration was calculated as averaged values of 5 measurements, collected on 6 different specimens for each different typology of substrate.

Static contact angle (CAs) was measured by the sessile drop method [28] using a conventional drop shape technique OCA 20 apparatus (DataPhysics Instrument GmbH, Filderstadt, Germany). To avoid any surface contamination, all specimens were rinsed in ethanol and accurately air-dried just before measurement [29]. Determination of CAs was based on the Young–Laplace equation. All CAs measurements were carried out at ambient condition before and immediately after UV irradiation. The result was the mean of the drop on ten replicate measurements, collected on 6 different specimens for each different typology of substrate.

The surface topography was examined by using the surface roughness tester (SAM TOOLS, by S.A.M.A.I., SA6200). The roughness characteristics were obtained from 5.0 x 5.0 cm^2 surface. Root mean square roughness, Rq, mean peak to valley height roughness, Rz, and arithmetic average absolute values of the roughness, Ra, were calculated. The surface roughness was then calculated by choosing cut-off length of 2.5 mm for unglazed samples and 0.8 mm for glazed samples. In fact, measurements of surface roughness usually requires the selection of different cut-off lengths based on the roughness surface. In general, fine surfaces require short cut-off and rough surfaces a longer one. Five measurements were made on 6 different specimens for each different typology of substrate.

To verify the mechanical properties of the coatings, scratch tests (Micro-Combi tester) with linearly increasing load (0.1 N to 6 N, scratch speed of 1 mm/min) were performed

on the glazed samples using a Rockwell indenter with spherical tip, 200μm radius. At least three scratches with the minimum distance between two scratches set at 4 mm were performed on 6 different specimens for each different typology of substrate, to achieve representative results of the average response for wider surfaces.

The microstructure of the sample surfaces was studied by scanning electron microscopy (FEI ESEM Quanta 200, USA) and analyzed by energy dispersive X-ray spectroscopy to confirm the presence of titania.

3. Results and discussion

3.1 Aesthetical properties

In Table 3 ΔE* between the coated surfaces and the untreated sample is reported. The results showed that after the application of the TiO_2-SiO_2 coating on the unglazed samples, the surfaces were slightly modified. In particular, in all samples a small decrease in the L* values and a slight increase in b* values occurred due to the presence of titania nanoparticles in the coating. This behavior was particularly evident for the coatings obtained at 300°C (PT_{300} and PT_{300}/Ag samples). However, the measured color variations, ΔE*, were moderate and acceptable (2.4 and 3.1, respectively). Indeed, according to Italian guidelines for the restoration of stone buildings, ΔE* after an intervention must be less than 5 [30] to be transparent to human eyes.

Regarding the glazed samples, the data reported in Table 3 for the titania coated samples were comparable with that obtained on untreated materials underlining the high transparency of the coating. Instead, the silver addition involved a higher decrease in the L* values and the PTg_{150}/Ag and PTg_{300}/Ag samples appeared slightly darker than Pg sample. However, the measured ΔE* values, also in this case, were moderate and acceptable being always below 5 (3.4 and 3.5 for PTg150/Ag and PTg300/Ag samples, respectively). Similar results can be found in literature, i.e, when TiO_2-SiO_2 and TiO_2

9

solutions were applied on limestones and clay bricks producing an acceptable ΔE^* of 4.51±1.82 and 5.57±0.80, respectively [13, 22].

3.2 Microstructural analysis

In Figure 1, the SEM images of unglazed and glazed samples before titania-silica coating deposition are reported. The image of the P sample (Figure 1a) showed the presence, as expected, of heterogeneous porosity. On the other hand, the image of the Pg sample (Figure 1b) showed an homogeneous surface due to the vitreous enamel that completely covered and closed the support porosity. In Figure 2, the SEM images of the coated samples are reported. The image of the PT_{300} sample, chosen as representative (Fig. 2a), showed a decrease of the small porosity due to the nanostructured coating that is, however, unable to close the big pores. The SEM image in Fig. 2b illustrated the close resemblance in the morphology of the glazed sample after TiO_2-SiO_2 deposition. In both samples, EDS analyses reported in Figure 3 confirmed that TiO_2 phase is present on the surfaces, after TiO_2-SiO_2 deposition.

Although the SEM analysis did not allow an evaluation of the different morphology after the nanostructured coating addition, the roughness data (Table 4) underline the smoothing effect of the coatings on Pg sample. In fact, the root mean square roughness, R_q, the arithmetic average absolute value, R_a and the peak-to-valley-height roughness, R_z were 4.38, 4.30 and 12.16 μm for the glazed sample (Pg). Addition of TiO_2-SiO_2 coating led to lower values of surface roughness parameters (R_a, R_q, R_z), for example R_a was 2.46, 2.16 and 2.88 μm for the samples PTg_{25}, PTg_{150} and PTg_{300} (see Table 4). When silver was added in the coating, this behaviour did not change and the PTgx samples (where "x" defines the different treatment temperatures, 25, 150 and 300°C) had always lower roughness parameters (i.e. R_a was 1.62, 1.58 and 3.71 μm for the samples PTg_{25}/Ag, PTg_{150}/Ag and PTg_{300}/Ag) if compared with Pg sample.

10

While the TiO_2-SiO_2 coated glazed surfaces resulted in smoother surfaces as compared to untreated glazed sample, the coated unglazed samples, both with and without silver addition, had surface roughness values higher than the untreated unglazed sample (P), although characterized by higher standard deviations. Considering that the nanocoating (nm) influenced the roughness of the samples, whereas there are three different orders of magnitude, these results can be probably associated to the initial roughness and porosity of specimen surfaces. In fact in the unglazed samples, the nanostructured coatings, as confirmed by SEM images (Fig. 2b), were not able to cover the porosity and thus to create a homogeneous and continuous film, but further investigations are needed.

3.3 Scratch resistance

In order to verify the adhesion and the mechanical durability of the coatings, scratch tests, with linearly increasing load, were performed on samples with higher self-cleaning discoloration and lower porosity (glazed samples). In general, the obtained results (Figure 4) show that the deposition of the nanostructured coatings allows an increase of the scratch resistance as underlined by the decrease of the penetration depth both on PTg_x and PTg_x/Ag samples, where "x" defines the different treatment temperatures (25, 150 and 300°C). Moreover, as the temperature is increased, a decrease of Pd values, attributed to a high structural integrity of the coatings related to the temperature of the thermal treatment, is observed. In fact the slope of the penetration curves decreases progressively with the increase of the thermal treatment temperature. Similar scratch results were obtained in literature demonstrating that the scratch resistance of sol-gel coating deposited on ceramic tiles increases as temperature is increased [18, 31]. The abrupt change in the penetration depth curve of the sample

11

PTg_{25} at higher load could be related to detachment of the coating during the scratch test [32].

In the case of PTg_{25}/Ag and PTg_{150}/Ag samples (Figure 4) a decrease of penetration resistance was noted in terms of penetration depth (Pd) with respect to the sample PTg_{300}/Ag. This is attributable to their lower surface roughness, as showed in Table 4. Infact, as reported by several works [33, 34], surface characteristics and material parameters can have significant effects on scratch behaviour. In particular, the friction force, strongly dependant on surface roughness, leads to a compressive stress to the front edge of the contact and then intensify the tensile stress at the back edge with fracture events.

3.4 Surfaces photocatalytic properties

To evaluate the photocatalytic activity of the obtained coatings UNI 11259 test was performed [26]. In Figure 5 R(t) values are reported for all the samples. It can be noted that also the untreated samples (Pg and P) have a slightly color variation due to the degradation effect of the UV light on the RhB. This bleaching of dye under visible/UV light can be associated with the absorption of light in the 350-520 nm range. However, all the coatings, except PTg_{300}/Ag(R4) and PT_{300}/Ag(R26), have a higher specific photoactivity with respect to the untreated ceramic materials.

On the glazed samples (Figure 5a), at the end of 4 hours, the red color of RhB had lost at least about 65-70% of its intensity up to a maximum of almost 80% for the PTg_{300} sample. Increasing the UV irradiation time, the R(26) values increased but they were not higher than 80%. The stain photodegradation was clearly faster during the first hours of UVA light exposure and, after 26 hours of exposure, the photodegradation values of glazed samples were independent on the temperature of the thermal treatment. These results are in good agreement with results reported in other research works. For

12

ACCEPTED MANUSCRIPT

exemplum, Bergamonti et al. demonstrated that on Comiso and Modica limestone samples treated with titania based sol-gel coatings, the dye photodegradation is very high (about 70%) in the first few hours of exposure [30].

Regarding the silver addition the results clearly showed that the photodegradation efficiency under UV light decreased being the obtained R(26) values not higher than 70%. On the unglazed samples (Figure 5b), probably due to the high surface porosity of the substrate, the effect of the thermal treatment of the coating is more visible. In fact the photocatalytic efficiency of the samples increased as the temperature was increased due to the higher conversion of the sol-gel coating at higher temperature that allows to create a more compact film on the substrate. Also in this case, the silver addition inhibited the photocatalytic activity that was not higher than 60% in all the studied conditions.

In the present study the effect of silver addition on both glazed and unglazed samples is in contrast with the results reported in literature that showed as Ag nanoparticles, in general, do not alter the photocatalytic efficiency of titania [23]. This behaviour can be attributed to competitive UV absorption reactions between silver ion and titania. In fact, is well known that, when irradiated by UV light also in presence of titania [35], Ag+ is reduced to Ag° decreasing the amount of UV light that can be absorbed by titania. Following the UNI11259 rule, however, it is important to notice that almost all the obtained samples can be considered photocatalytic being the R(4) values higher than 20% and R(26) values higher than 50%. The only exception is PT_{300}/Ag R(26) even if it is quite close to the minimum requested value by taking into account its standard deviation (Fig. 5b). In particular, even if UV light was able to produce a dyes decomposition, the discoloration produced by the photocatalytic action of TiO_2-SiO_2

coating was in general higher underling as our TiO_2-SiO_2 coating is able to increase the kinetic of the process when it is applied on ceramic substrate.

The wetting properties of the obtained surfaces in terms of static water CAs, were also determined (Table 4). For the unglazed samples, CAs of 0° were measured even on the coated samples. It can be deduced that the contribution of titania coatings, with or without silver addition, was negligible with respect to the sample surface porosity. However, the contribution from titania-silica sol should not be overlooked for the glazed-samples. For example, PTg_{25} sample had the lower CAs among the treated sample. A contribution from hydroxyl groups could in principle be present in PTg_{25}. In fact, comparing the CAs values of PTg_{150} and PTg_{300}, it can be concluded that after the thermal treatment there was a densification of the silicon-oxide skeleton with a decrease/elimination of hydroxyl contents as already reported in Bondioli et al.[31]. The photo induced hydrophilicity of coated and uncoated surfaces was verified through contact angle measurements after 30 min of UV-light irradiation (Table 4). Photoinduced hydrophilic surfaces are observed in the samples PTg_{25}, PTg_{150} and PT_{150}/Ag. In these samples the contact angle decreases significantly after 30 min of UV-light irradiation reaching values of 9-12°. No change of the contact angle was observed in the others samples as a function of UV-light irradiation. The results suggest that the photoinduced hydrophilicity of the titania-silica films is closely correlated with the annealing temperature. Also in this case, as already discussed for the photocatalytic test, the silver addition seems to inhibit the photoinduced activity of the coatings on glazed samples expect for the sample PTg_{150}/Ag that is however characterised by a very low surface roughness (Table 4).

According to these results, we can conclude that, even if the nanostructured coating gives to both unglazed and glazed samples photocatalytic properties, is not able to

completely cover the highly porous substrate of the unglazed samples making necessary the glazing step. Moreover, the best sample was found to be PTg_{150} because the coating is transparent and well bonded to the substrate and the sample has a good discoloration efficiency of dye solution and a very fast photoinduced hydrophilicity.

4. Conclusions

A titania-silica based coating, obtained by sol-gel technique, was used in this work to improve the surfaces properties of a new green material based on huge amount of packaging glass waste for use as wall or floor coverings.

This study investigated the effect of several thermal treatments and $AgNO_3$ presence, mainly the photocatalytic efficiency of TiO_2-SiO_2 coating and scratch resistance.

The results showed that, with the proper thermal treatment, good photocatalytic activity, and scratch resistance can be obtained. The best surface properties are found after thermal treatment at 150°C. The color difference before and after the treatments is acceptable and the coatings are crack–free. Even if the silver addition could assure antibatteric properties in any illumination conditions, the presence of $AgNO_3$ decreases the sample photoactivity. Finally, the obtained results showed that to improve the material cleanability the glaze layer is necessary because the nanostructured coating is not able to completely cover the porous substrate. Regarding the efficiency of the nanostructured coating, performances (cleanability, scratch resistance, photocatalytic activity) are comparable with that of self-cleaning traditional ceramic tile products already on the market and with that obtained, with the same coating, on different substrates (limestone, bricks,….).

In conclusion, the new ceramic material, developed here through a surface cleanability enhancement using a titania-silica sol, can represent a novel sustainable construction

product, reducing the amounts of waste disposed in landfills, the consumption of raw

materials and the energy costs.

Acknowledgements

References

[1] A.C. Warnock, An overview of integrating instruments to achieve sustainable construction and buildings, Manag. of Environ. Qual. 18 (2007) 427-441.

[2] M. Pitt, M. Tucker, M. Riley, J. Longden, Towards sustainable construction: promotion and best practices, Constr. Innovat. 9 (2009) 201.

[3] J. Pinkse, M. Dommisse, Overcoming barriers to sustainability: an explanation of residential builder reluctance to adopt clean technologies, Bus. Strategy Environ. 18 (2008) 515-527.

[4] A. Sev, How Can the Construction Industry Contribute to Sustainable Development? A Conceptual Framework, Sustain Dev. 17 (2009) 161-173.

[5] I. Holton, I. Glass, A.Price, Developing a successfull sector sustainability strategy: six lessons from the UK construction products industry, Corp. Soc. Responsab. Environ. Manag. 15 (2007) 29-42.

[6] Co.Re.Ve, (2014), Part of the Specific Prevention Plan 2014 (Parte del Piano Specifico di Prevenzione 2014). Risultati di Raccolta e Riciclo 2013, On line at: http://www.reloaderitalia.it/documents/download/documenti_studi/2014/italia_del_ricic lo_2014_schede sintetiche.pdf.

[7] C.Leonelli, L. Barbieri, F. Andreola, E.Reggiani, M.Ingrami, Glass based material for the production of ceramic products and method for its preparation (Materiale a base vetrosa per la produzione di manufatti ceramici e metodo per la sua preparazione), 2011 italian Patent application MI2011A000369, 2013 Patent certificate for industrial invention n. 0001404410, University of Modena and Reggio Emilia.

[8] R. Taurino, F. Andreola, L. Barbieri, C. Leonelli, A. Vallini, N. Campani, Recycled glass waste in Italy for achieving environmental sustainability, in: I.G. Ivan Nishkov,

Dimitar Mochev (Ed.) XV Balkan MIneral Processing CongressSozopol, Bulgaria, 2013, pp. 869-870.

[9] A.P. Luz, S. Ribeiro, Use of glass waste as new material in porcelain stoneware tile mixtures, Cer. Int. 33 (2007) 761-765.

[10] A. Tucci, L. Esposito, E. Rastelli, C. Palmonari, E. Rambaldi: Use of soda-lime scrap-glass as a fluxing agent in a porcelain stoneware tile mix, J. Eur. Cer. Soc. 24 (2004) 83-92.

[11] L. Esposito, E. Rambaldi, A. Tucci, Recycle of Waste Glass into "Glass-Ceramic stoneware", J. Am. Ceram. Soc. 91 (2008) 2156-2162.

[12] C. Sciancalepore, T. Manfredini, F. Bondioli, Antibacterial and self-cleaning coatings for silicate ceramics: a review, Adv. Sci. Tech. 92 (2014) 90-99.

[13] L. Graziani, E. Quagliarini, F. Bondioli, M. D'Orazio, Durability of self-cleaning TiO_2 coatings on fired clay brick facades: Effects of UV exposure and wet & dry cycles, Build. Environ. 71 (2014) 193-203.

[14] J. Chen, C.S. Poon, Photocatalytic construction and building materials: From fundamentals to applications, Build. Environ. 44 (2009) 1899-1906.

[15] A. Fujishima, K. Honda, Electrochemical photolysis of water at a semiconductor electrode, Nature. 238 (1972) 37-38.

[16] J. Zhao, X.D. Yang, Photocatalytic oxidation for indoor air purification: a literature review, Build. Environ. 38 (2003) 645-654.

[17] M.V. Diamanti, B. Del Curto, M. Ormellese, M.P. Pedeferri, Photocatalytic and self-cleaning activity of colored mortars containing TiO2, Constr. Build. Mater. 46 (2013) 167-174.

[18] C. Sciancalepore, F. Bondioli, Durability of SiO_2-TiO_2 photocatalytic coatings on ceramic tiles, Int. J. Appl. Ceram. Technol. 12 (2015) 679-684.

19

[19] X.J. Zhao, Q.N. Zhao, J.G. Yu, B.S. Liu, Development of multifunctional photoactive self-cleaning glasses, J. Non-Cryst Solids. 354 (2008) 1424-1430.

[20] E. Quagliarini, F. Bondioli, G.B. Goffredo, A. Licciulli, P. Munafo, Smart surfaces for architectural heritage: Preliminary results about the application of TiO_2-based coatings on travertine, J. Cult. Herit. 13 (2012) 204-209.

[21] I.G. Marino, R. Raschella, P.P. Lottici, D. Bersani, C. Razzetti, A. Lorenzi, A. Montenero, Photoinduced effects in hybrid sol-gel materials, J. Sol-Gel Sci. Techn. 37 (2006) 201-206.

[22] L. Pinho, M.J. Mosquera, Photocatalytic activity of TiO_2-SiO_2 nanocomposites applied to buildings: Influence of particle size and loading, Appl. Catal. B: Environ. 134-135 (2013) 205-221.

[23] S. de Niederhausern, M. Bondi, F. Bondioli, Self-Cleaning and Antibacteric Ceramic Tile Surface, Int. J. Appl. Ceram. Technol. 10 (2013) 949-956.

[24] R. Taurino, E. Fabbri, M. Messori, F. Pilati, D. Pospiech, A. Synytska, Facile preparation of superhydrophobic coatings by sol-gel processes, J. Colloid Interf. Sci. 325 (2008) 149-156.

[25] N. M. Dmitriev, Surface porosity and permeability of porous media with a periodic microstructure, Fluid Dynam. 30 (1995) 64-69.

[26] UNI EN 15801:2010, Conservation of cultural property - test methods - colour measurement of surfaces, 2010.

[27] UNI EN 11259:2008, Determination of the photocatalytic activity of hydraulic binders Rodammina test method, 2008.

[28] T.H. Muster, C.A. Prestidge, Application of Time-Dependent Sessile Drop Contact Angles on Compacts to Chracterise the Surface Energetics of Sulfathiazole Crystal, Int. J. Pharm. 234 (2002) 43-45.

[29] M. Maeda, S. Yamasaki, Effect of Silica Addition on Crystallinity and Photo-Induced Hydrophilicity of Titania-Silica Mixed Films Prepared by sol-gel Process, Thin Solid Films. 483 (2005) 102-106.

[30] L. Bergamonti, I. Alfieri, A. Lorenzi, A. Montenero, G. Predieri, G. Barone, P. Mazzoleni, S. Pasquale, P.P. Lottici, Nanocrystalline TiO_2 by sol-gel: Characterisation and photocatalytic activity on Modica and Comiso stones, Appl. Surf. Sci. 282 (2013) 165-173.

[31] F. Bondioli, R. Taurino, A.M. Ferrari, Functionalization of ceramic tile surface by sol-gel technique, J. Colloid Interf. Sci. 334 (2009) 195-201.

[32] T.H. Zhong, Y. Huan, Nanoindentation and nanoscratch behaviors of DLC coatings on steel substrates, Comp.Scie.Tech., 65 (2005) 1409-1413.

[33] H. Jiang, R. Browing, J.Fincher, A. Gasbarro, S. Jones, H.J. Sue, Influence of surface roughness and contact load on friction coefficient and scratch behaviour of thermplastic oleofins, Appl. Surf. Sci. 254 (2008) 4494-4499.

[34] A. Krupička, M. Johansson, A. Hult, Use and interpretation of scratch tests on ductile polymer coatings, Prog. Org. Coat. 46 (2003) 32-48.

[35] K. Naoi, Y. Onko, T. Tatsuma, TiO2 films loaded with silver nanoparticles: control of multicolor photocromic behavior, J. Am. Chem. Soc. 126 (2004) 3664-3668.

Figure captions

Figure 1. SEM images of P (a) and Pg (b) samples (top view).

Figure 2. SEM images of PT_{300} (a) and PTg300 (b) samples (top view), chosen as representative.

Figure 3. SEM images and EDS spectra of PT_{300} (a) and PTg_{300} (b) samples.

Figure 4. Average values of penetration depth (Pd) in a progressive load scratch test on PTg_x and PTg_x/Ag samples.

Figure 5. Average values and standard deviation of photoinduced discoloration, R(t), on a) PTg_x, PTg_x/Ag, and b) PT_x, PT_x/Ag samples after 4 and 26 hours of UV exposure.

Tables

Table 1. Composition of the titania-silica solution gently furnished by NextMaterials

s.r.l.

Element	Concentration (wt%)
Water	93
Titanium dioxide	2
Functionalized silica	2
Isopropyl-alcohol	<3
Acetic acid	<1
Nitric acid	<1
Methyl-alcohol	<0.5

Table 2. Composition of the prepared samples, including heat temperature, time and

amount of $AgNO_3$ applied on unglazed (P) and glazed (Pg) ceramic surfaces

Sample ID	$AgNO_3$ [g/l]	Heat temperature (°C)	Treatment time
P	Untreated unglazed ceramic sample		
PT_{25}	0	25	24h
PT_{150}	0	150	15 min
PT_{300}	0	300	15 min
PT_{25}/Ag	0.25	25	24h
PT_{150}/Ag	0.25	150	15 min
PT_{300}/Ag	0.25	300	15 min
Pg	Untreated glazed ceramic sample		
PTg_{25}	0	25	24h
PTg_{150}	0	150	15 min
PTg_{300}	0	300	15 min
PTg_{25}/Ag	0.25	25	24h
PTg_{150}/Ag	0.25	150	15 min
PTg_{300}/Ag	0.25	300	15 min

Table 3. Average value and standard deviation of color parameters and color change,

(ΔE^*), due to the treatments on unglazed and glazed tiles.

Sample ID	L*	a*	b*	ΔE^*
P	80.35±0.50	3.43±0.10	15.02±0.21	/
PT_{25}	79.50±1.26	3.54±0.08	15.72±0.43	1.11
PT_{150}	80.22±0.29	3.49±0.14	15.35±0.36	0.36
PT_{300}	78.87±0.56	3.65±0.20	16.84±0.31	2.36
PT_{25}/Ag	79.85±0.77	3.50±0.21	15.49±0.34	0.69
PT_{150}/Ag	80.52±0.56	3.35±0.12	15.51±0.25	0.53
PT_{300}/Ag	77.25±0.34	3.63±0.21	15.32±0.39	3.12
Pg	76.58±1.60	2.69±0.16	16.32±0.47	/
PTg_{25}	76.13±0.57	2.83±0.31	16.35±0.29	0.47
PTg_{150}	75.18±0.31	2.67±0.08	16.72±0.41	1.46
PTg_{300}	75.93±0.34	2.63±0.09	17.12±0.26	1.03
PTg_{25}/Ag	74.50±1.19	2.43±0.09	16.11±1.20	2.11
PTg_{150}/Ag	73.22±0.46	2.35±0.08	16.00±0.32	3.39
PTg_{300}/Ag	73.05±0.33	2.52±0.03	16.56±0.12	3.54

Table 4. Average value and standard deviation of static water CAs at t=0 (θ_S) and after 30 min of UV irradiation (θ_S-UV), and roughness parameters (Rq, Rz, Ra,) of the obtained samples.

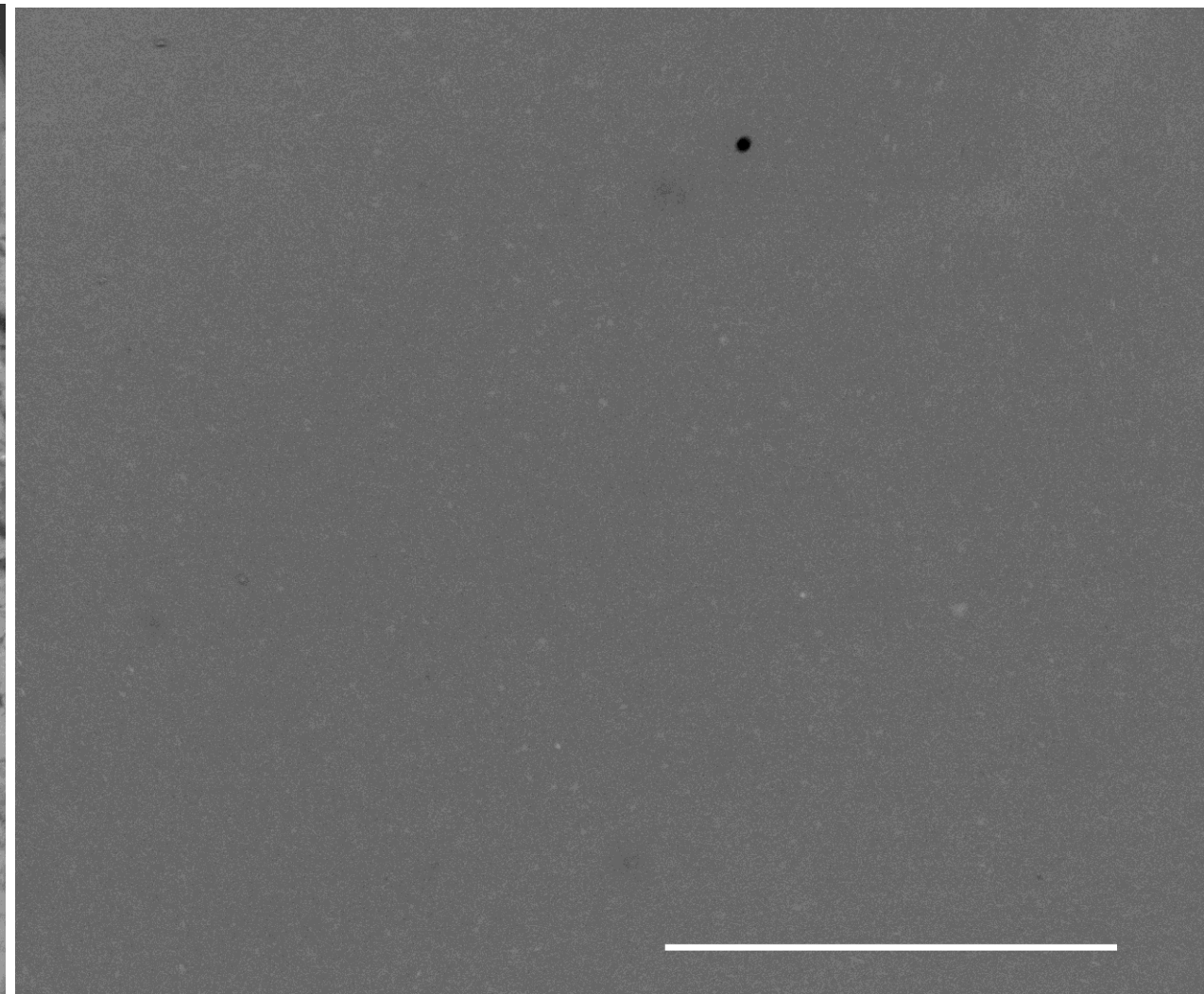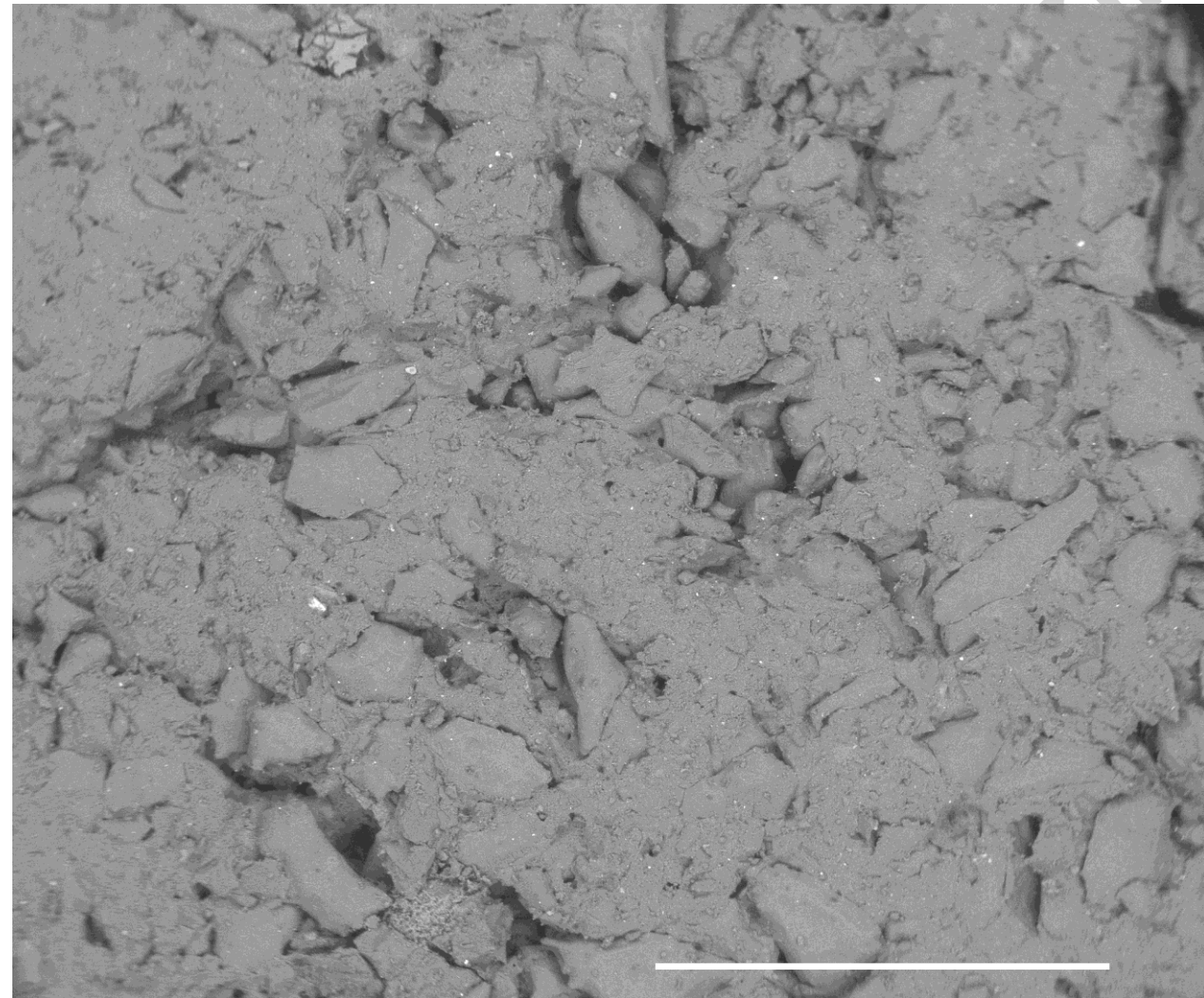| Sample ID	θs(°)	θs-UV(°)	Ra(μm)	Rq(μm)	Rz(μm)
P	0	0	16.5±3.5	17.5±2.1	49.4±5.9
PT_{25}	0	0	20.1±2.0	20.9±3.1	59.2±8.7
PT_{150}	0	0	17.6±0.5	17.5±0.5	55.6±9.7
PT_{300}	0	0	20.6±0.3	20.2±0.6	57.3±1.6
PT_{25}/Ag	0	0	24.1±2.3	23.2±3.1	56.1±5.6
PT_{150}/Ag	0	0	19.6±2.5	20.5±1.8	60.6±6.7
PT_{300}/Ag	0	0	22.8±1.3	24.2±0.8	58.4±2.6
Pg	17.73±2.21	16.94±1.92	4.30±0.31	4.38±0.45	12.16±1.62
PTg_{25}	31.05±5.05	10.45±3.89	2.46±0.06	2.51±0.12	6.95±0.16
PTg_{150}	67.20±1.59	11.86±4.30	2.16±0.03	2.12±0.07	6.10±0.08
PTg_{300}	40.08±4.10	37.40±2.69	2.88±0.12	2.95±0.08	8.17±0.34
PTg_{25}/Ag	29.53±5.94	26.65±9.23	1.62±0.17	1.65±0.12	4.57±0.49
PTg_{150}/Ag	61.77±1.48	9.95±1.91	1.58±0.16	1.66±0.20	4.47±0.45
PTg_{300}/Ag	44.50±8.62	40.30±7.92	3.71±0.84	3.72±0.93	10.49±2.36
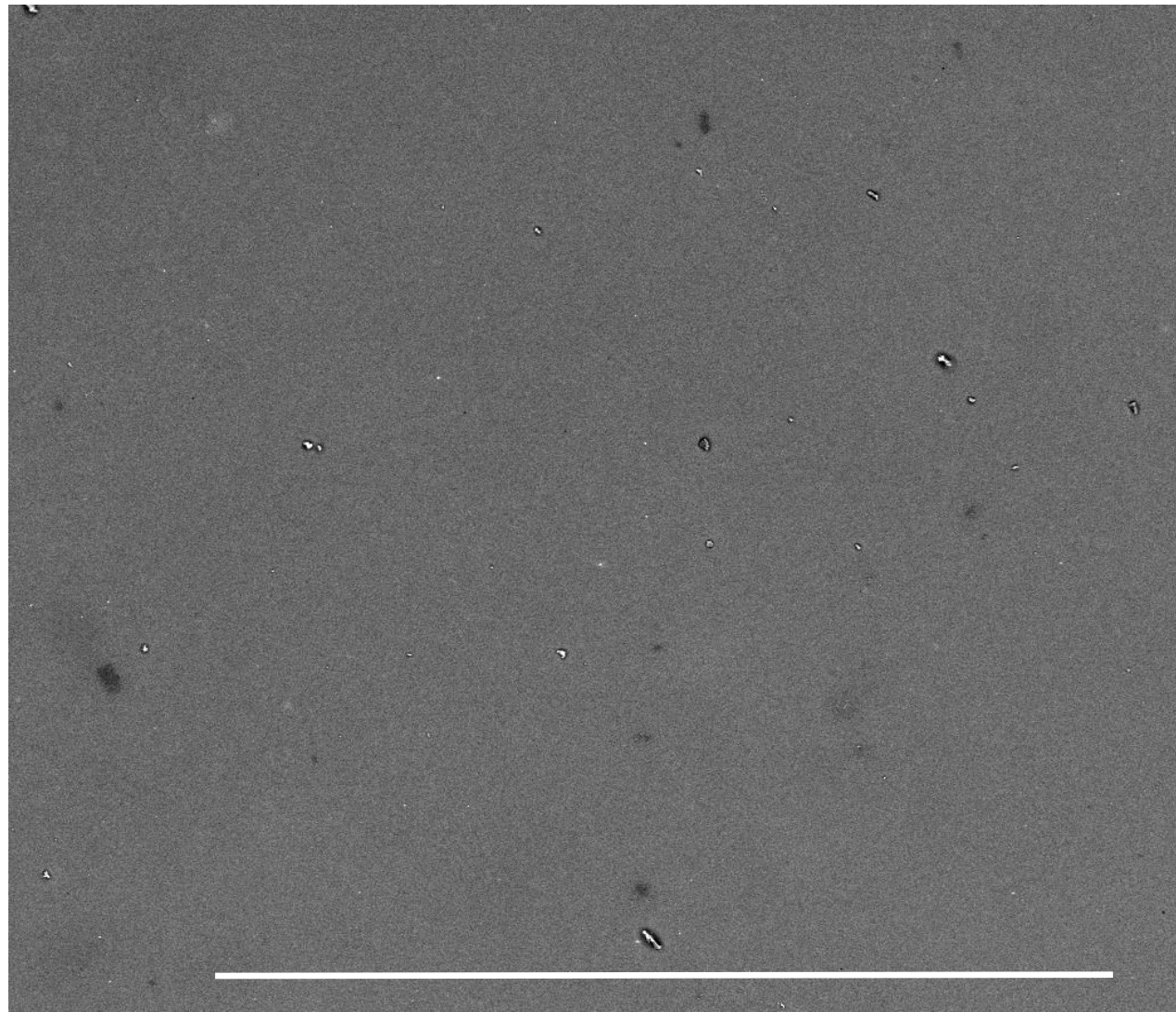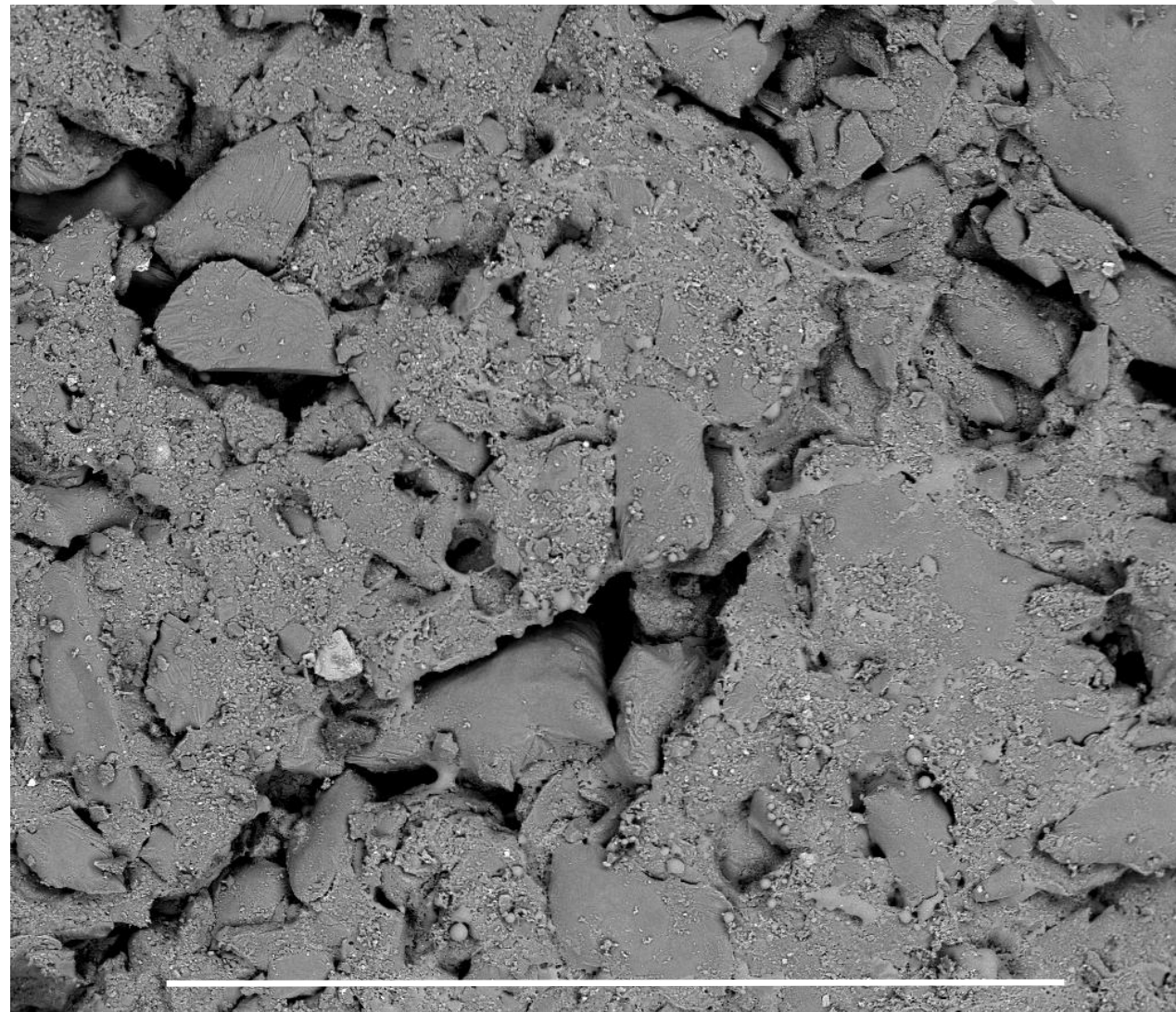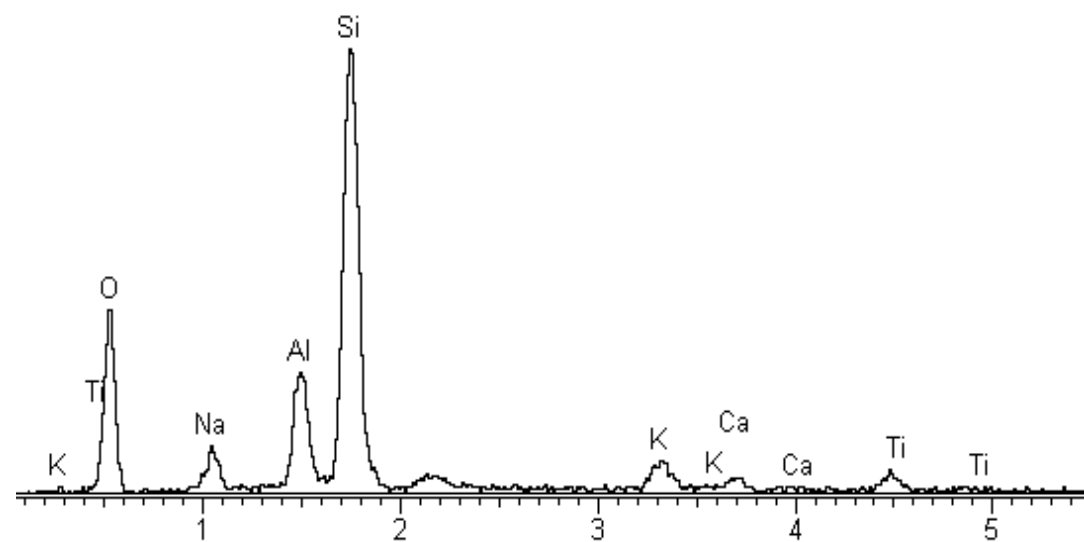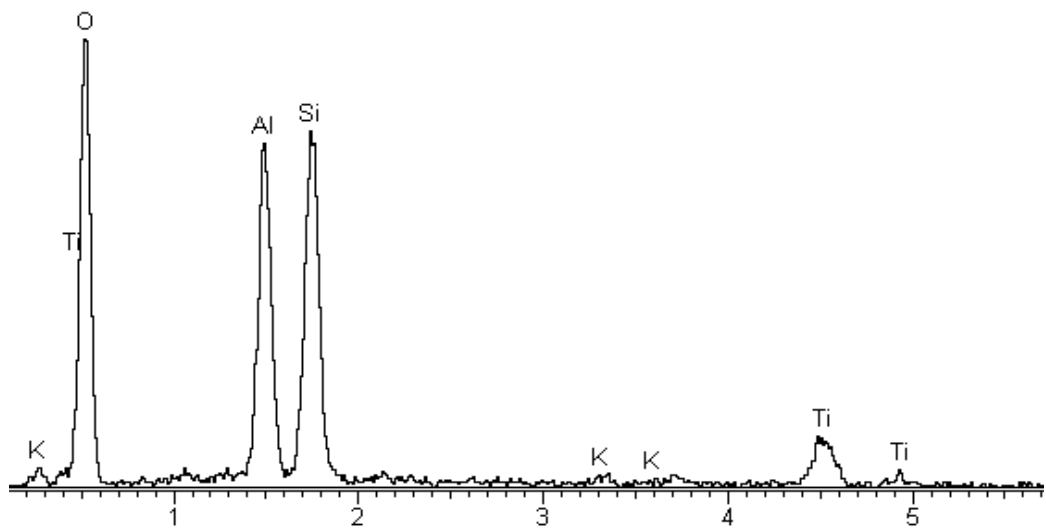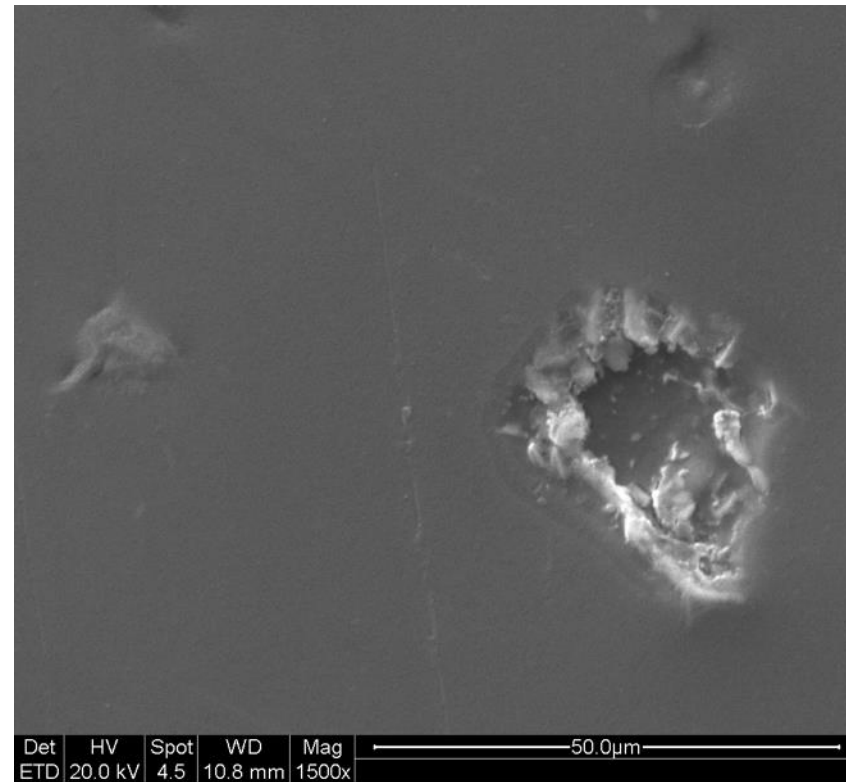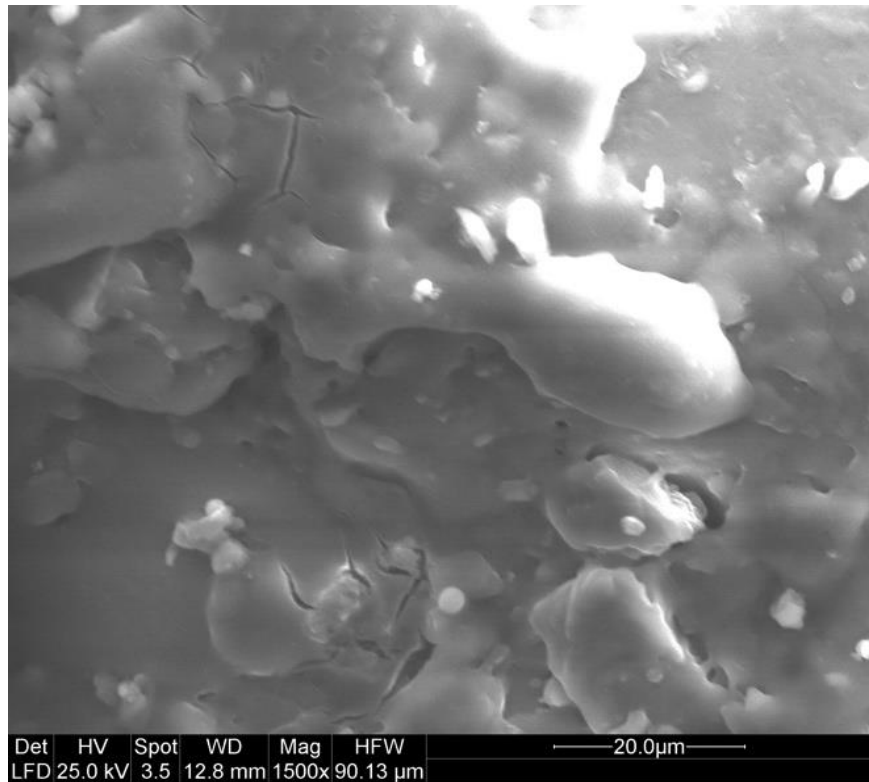
a) R(t) vs samples (Pg, PTg25, PTg150, PTg300, PTg25/Ag, PTg150/Ag, PTg300/Ag) for R4 and R26

b) R(t) vs samples (P, PT25, PT150, PT300, PT25/Ag, PT150/Ag, PT300/Ag) for R4 and R26